

USING TIGGE DATA TO DIAGNOSE INITIAL PERTURBATIONS AND THEIR GROWTH FOR TROPICAL CYCLONE ENSEMBLE FORECASTS

Munehiko Yamaguchi*
 Division of Meteorology and Physical Oceanography
 Rosenstiel School of Marine and Atmospheric Science
 University of Miami, Miami, Florida

1. INTRODUCTION

Many operational numerical weather prediction centers such as European Centre for Medium-Range Weather Forecasts (ECMWF), the National Centers for Environmental Prediction (NCEP), and Japan Meteorological Agency (JMA) operate ensemble prediction system (EPS) to extract useful information on the uncertainty of forecasts via the ensemble spread. While the validity of ensemble tropical cyclone (TC) track predictions has been verified in various EPSs, those predictions sometimes contradict each other. Figure 1 shows an example in which one EPS predicts relatively small ensemble spread while the other possesses large ensemble spread and vice versa. It is hypothesized that these differences are attributed to the different methods of creating initial perturbations, resulting in different growth of the perturbations. In addition, initial amplitudes of the perturbations may affect the size of the ensemble spread, especially in the early forecast stage. A systematic intercomparison of global model ensembles for TCs has hitherto been difficult because of the limited access to such operational data. However, the recently established THORPEX Interactive Grand Global Ensemble (TIGGE) database makes it possible to conduct an intercomparison study and verify such hypotheses as proposed above.

In this study, ensemble initial perturbations in and around Typhoon Sinlaku (2008), one of the typhoons heavily sampled during the THORPEX Pacific Asian Regional Campaign (T-PARC) and Tropical Cyclone Structure 2008 (TCS-08) field campaigns, are compared using the ECMWF, NCEP and JMA ensembles which are available on the TIGGE database; vertical and horizontal distributions of perturbation wind, temperature and specific humidity as well as their amplitudes are compared. Following this, the dynamical mechanisms of the perturbation growth are investigated by comparing the ECMWF and NCEP ensembles to understand how the perturbations change the steering flow and symmetric and asymmetric circulations of Sinlaku. Finally, a statistical verification is conducted to identify whether there exists a relationship between the ECMWF and NCEP ensemble spread of tracks during the 2007 and 2008 seasons and to establish how the initial perturbations and their growth affect the ensemble spread of tracks in each EPS.

* Corresponding author address: Munehiko Yamaguchi
 RSMAS/MPO, University of Miami
 4600 Rickenbacker Causeway, Miami, FL 33149
 email: myamaguchi@rsmas.miami.edu

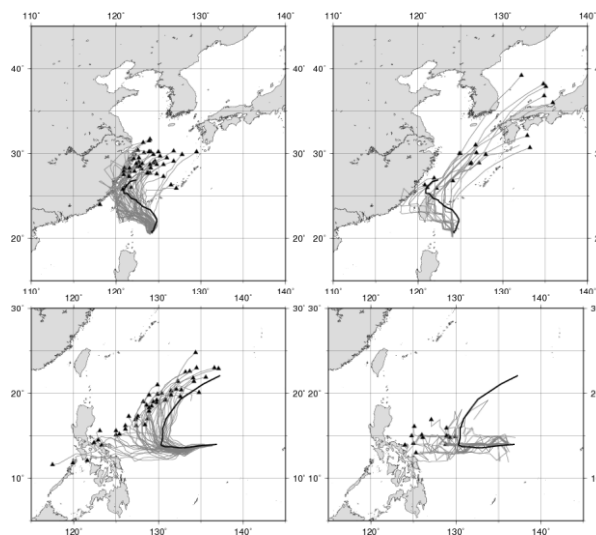


Fig.1. Ensemble track forecasts (gray lines) by the ECMWF (left) and NCEP (right) ensembles for Typhoon Sinlaku initialized at 1200 UTC of 10th September 2008 (top) and Typhoon Dolphin initialized at 0000 UTC of 13th December 2008 (bottom). The black line is the best track. The black triangles are the forecast positions at 120-h.

2. RESULTS

2.1. Vertical and horizontal distributions of the initial perturbations

The vertical and horizontal distributions of the initial perturbations as well as their amplitude are found to be quite different among the NWP centers. Figure 2 shows the vertical profiles of perturbation kinetic energy by the ECMWF, NCEP, and JMA ensembles for Typhoon Sinlaku before recurvature. The perturbation kinetic energy ($u^2 + v^2$) is calculated at each vertical level (see Fig. 2) and averaged over the all ensemble members over a 2000 km \times 2000 km domain centered on Sinlaku. For example, the amplitude of the wind perturbation in NCEP is larger than ECMWF, especially in the upper troposphere; 9.2 times as large as ECMWF at 200-hPa. Meanwhile, the amplitude of the wind perturbation in JMA is 0.24 ms⁻¹ at 700 hPa on average; a quarter of ECMWF at the same level. Those differences can be seen in the perturbation available potential energy and the specific humidity energy (not shown, see Yamaguchi and Majumdar 2010 for more details). The differences are also seen in the horizontal distributions (not shown).

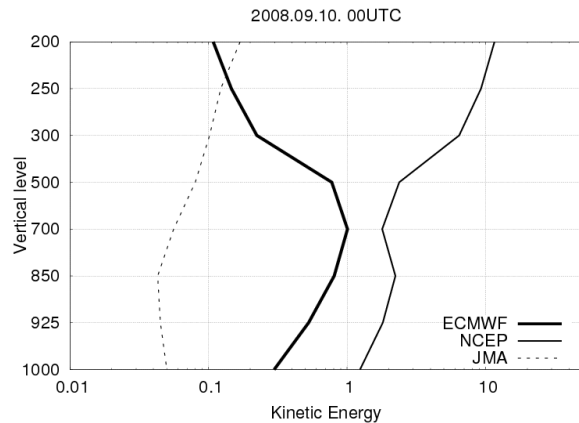


Fig. 2. Vertical distribution of kinetic energy component of initial perturbations around Typhoon Sinlaku before recurvature (2008.09.10.0000UTC) by the ECMWF, NCEP, and JMA ensembles.

It would be inferred that these differences cause the different modification of the TC motion at the initial time and subsequent forecast times. In Section 2.2, the evolution of the initial perturbations associated with Sinlaku's motion and how these perturbations modify the flow field of Sinlaku and its environment are examined.

2.2. Modification of the steering flow and symmetric and asymmetric circulations by perturbations

In principle, the total wind in the region of a TC can be decomposed into an environmental steering flow, a symmetric vortex and an asymmetric circulation (Carr and Elsberry 1992). The TC motion can be governed by 1) the steering flow associated with TC-background synoptic flow and 2) the asymmetric circulation which includes an azimuthal wavenumber one circulation like the beta gyres (e.g. Fiorino and Elsberry 1989). This section describes how the initial wind perturbation modifies the symmetric vortex of Sinlaku, the steering vector and the advection vector associated with the asymmetric circulation (hereafter referred to as asymmetric propagation vector), using the ECMWF and NCEP ensembles. In addition, the time evolution of the steering and asymmetric propagation vector is compared between the two ensembles.

Figure 3 shows the radial profile of the symmetric tangential wind at 850-hPa in the before-recurvature stage of Sinlaku by ECMWF and NCEP. The following four features can be seen in Fig. 3;

- 1) The size of the typhoon (radial profile of the symmetric tangential wind) is similar among the ensemble members in each EPS;
- 2) The range of the maximum tangential wind is less than 1 m s^{-1} ;
- 3) The radius of the maximum tangential wind does not change significantly;

- 4) The differences of the above three quantities between ECMWF and NCEP are much larger than the differences caused by the initial perturbations in each ensemble.

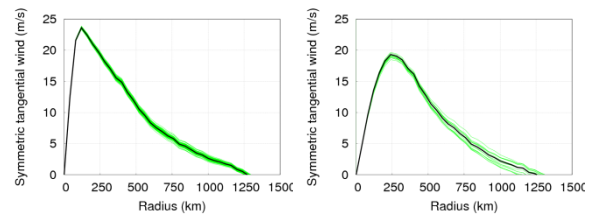


Fig. 3. Symmetric tangential wind at 850-hPa for Typhoon Sinlaku before recurvature produced by the ECMWF (left) and NCEP (right) ensembles. The black line is for the non-perturbed member and the green lines for the ensemble members.

Similar features are seen in the during- and after-recurvature stages and in 500-hPa wind field (not shown).

Figure 4 shows the modification and time evolution of the steering and asymmetric propagation vector by the ECMWF and NCEP perturbations for the before-recurvature stage of Sinlaku. The following four features can be seen in Fig.4;

- 1) The ECMWF ensemble shows the growth of the steering and asymmetric propagation vector while the NCEP ensemble does not;
- 2) The spread of the asymmetric propagation vector in ECMWF is larger than in NCEP;
- 3) Though the spread of the steering vector in ECMWF is smaller than that in NCEP at FT+0h, they become almost the same at FT+48h;
- 4) The growth of the steering and asymmetric propagation vector in ECMWF is larger in the early forecast period. The average perturbation wind magnitude of the steering (asymmetric propagation) vector is 0.37 (0.28), 1.04 (0.79), 1.06 (0.69), 0.94 (0.75) and 0.98 (0.86) ms^{-1} at 0, 12, 24, 36 and 48 hours, respectively.

Similar features are seen in the during- and after-recurvature stages.

The differences of the initial modification and growth of the steering and asymmetric propagation vector lead to the differences in the spread of ensemble TC track predictions between two ensembles. However, it remains to be seen what dynamical mechanisms cause the growth of the steering and asymmetric propagation vector in the ECMWF EPS. In Sections 2.3, the dynamical mechanisms that lead to the growth of perturbation kinetic energy in the ECMWF EPS are investigated.

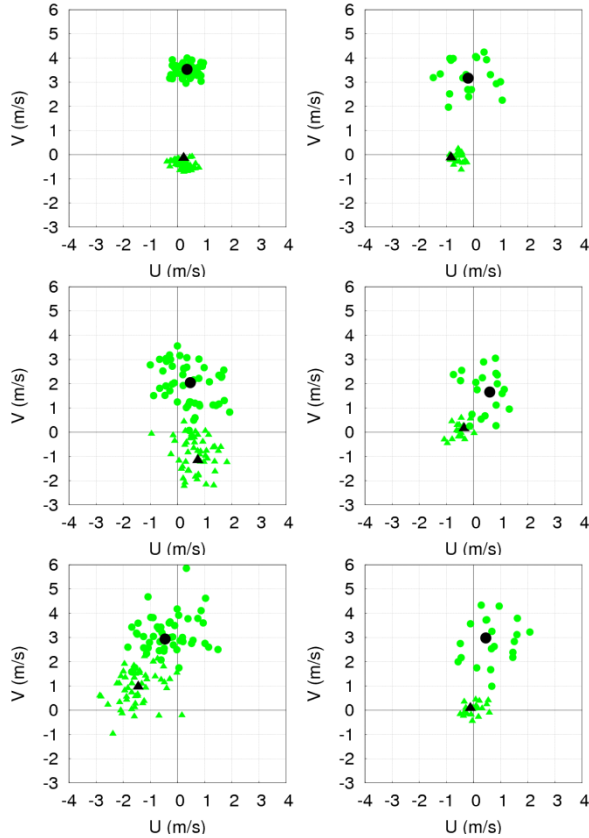


Fig. 4. Steering (circles) and asymmetric propagation (triangles) vector by the ECMWF (left) and NCEP (right) ensembles at FT+0h (upper), FT+12h (middle) and FT+48h (lower) for Typhoon Sinlaku before recurvature. The black (green) is for the non-perturbed member (ensemble members).

2.3. Dynamical mechanisms of the growth of the steering and asymmetric propagation vector

The ECMWF perturbations grow through 1) baroclinic energy conversion within a vortex, 2) baroclinic energy conversion associated with midlatitude waves, and 3) barotropic energy conversion within a vortex. Those features are found to be less distinctive in the NCEP ensemble. The dynamical mechanisms of (2) and (3) have been studied well while the mechanism for perturbations to grow through a baroclinic process and lead to the modification of the steering and asymmetric propagation vector is a relatively new concept. This section focuses on the baroclinic energy conversion mechanism in TCs (see Yamaguchi and Majumdar 2010 for the other two mechanisms).

The dynamics of baroclinic energy conversion in the mid-latitude waves can be applied to a TC-like vortex in a cylindrical coordinate system. The upper left in Fig. 5 shows the schematic to illustrate the baroclinic energy conversion in a vortex. In the case of the mid-latitude dynamics, the \times mark and the circle centered at the mark represent the north pole and a certain latitude,

respectively, while in the case of a vortex, they represent a TC center and a circulation at a certain radius, respectively. The only difference between the mid-latitude and a vortex is the background temperature gradient; the north is colder than the south in the mid-latitude while the TC center is warmer than the outer region (not shown). Thus, in the vortex case, a temperature perturbation (wave perturbation) needs to be 90 degrees ahead of a streamfunction perturbation so that the perturbation can obtain available potential energy from mean available potential energy.

The figures on the right in Fig. 5 are equivalent to the figures on the left; streamfunction (shade) and temperature (contour) perturbations at 500 hPa by ECMWF ensemble member 21 for the before-recurvature stage (upper), corresponding azimuthal structures at 500 km from the center of Sinlaku (middle), and the radial heat flux (lower). It is found that the azimuthal mean available potential energy will be converted into the eddy available potential energy from southwest to northeast of Sinlaku, with its peak at around south and east of Sinlaku.

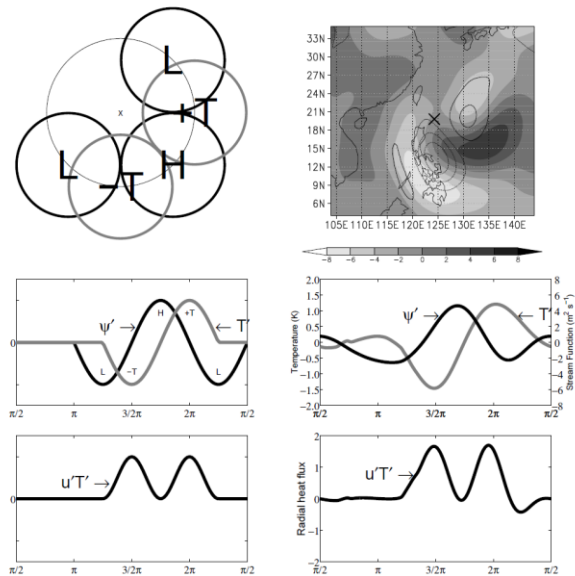


Fig. 5. Left: Schematic of horizontal map of streamfunction (ψ') and temperature (T') perturbations in a cylindrical coordinate system centered at a storm center (upper), corresponding azimuthal structures (middle) and the radial heat flux (lower). Right: Horizontal map of streamfunction (shade, divided by 100000) and temperature (contours, every 0.5 K, negative: dash lines, positive: solid lines, zero contour omitted) initial perturbations at 500 hPa by ECMWF ensemble member 21 for the before-recurvature stage of Typhoon Sinlaku (upper), corresponding azimuthal structures at 500 km from the storm center (middle) and the radial heat flux (lower). The \times mark in the upper right is the central position of Sinlaku.

Figure 6 shows the six-hourly time evolution of the wind perturbation (left), the azimuthal structures of streamfunction and temperature perturbations at 500 km from the center of Sinlaku (middle) and the radial heat flux (right). Note that the wind field of the non-perturbed member and ensemble member 21 is shifted to a storm-relative coordinate at each verification time. It is found that where the wind perturbation grows well corresponds to the region where the radial heat flux is positive, especially south and east of Sinlaku. As seen in the flow over the center of the storm, the growth of the wind perturbation leads to the change in the advection flow of Sinlaku. As a result of the significant modification of both the steering and asymmetric propagation vectors, the track of ensemble member 21 becomes one of the most different tracks from that of the non-perturbed member (not shown).

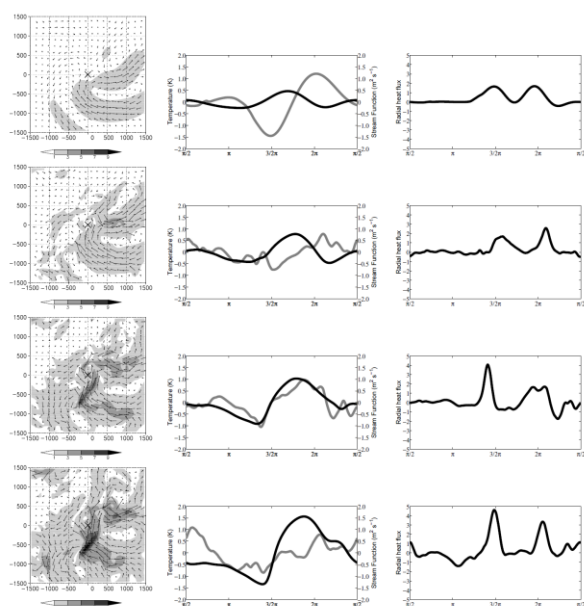


Fig. 6. Six hourly time evolution (FT+0h to FT+18h from up to bottom) of wind perturbations (ms^{-1}) at 500 hPa by ECMWF ensemble member 21 for the before-recirculation stage of Typhoon Sinlaku (left), the azimuthal structure of streamfunction (black lines, divided by 1000000) and temperature (gray lines) perturbations at 500 km from the storm center (middle) and the radial heat flux (right). Wind perturbations are described in a domain of 3000 km \times 3000 km centered at the storm center.

The perturbation structures capturing a baroclinic energy conversion process are not unique to ensemble member 21, but are common features for many ensemble members. However, they become less distinctive at the during- and after-recirculation stage of Sinlaku when the TC is more influenced by the midlatitude waves.

2.4. Evolution of ensemble spread of tracks in 2007 and 2008 seasons.

In order to compare quantitatively how the initial perturbations and their growth affect the ensemble spread of tracks in the ECMWF and NCEP EPS, a statistical relationship between their respective spreads of ensemble track predictions is examined for the 2007 and 2008 seasons. Figure 7 shows the verification results for 1-day (top) and 3-day (bottom) forecasts of the 2007 (left) and 2008 (right) seasons. The verification only includes TCs whose intensity is tropical storm or stronger. First, the correlation of the spread between the ECMWF and NCEP ensembles is found to be weak. The correlation coefficient of 1-day forecasts is 0.26 and 0.27 in 2007 and 2008 while that of 3-day forecasts is 0.56 and 0.21, respectively. The low correlation may arise due to the different methods of creating initial perturbations in the respective ensembles, as well as their respective differences in initial amplitudes and the growth of ensemble perturbations as presented above. Second, NCEP's spread for 1-day forecasts is larger than ECMWF on average. This can be attributed to the fact that the spread in the initial steering wind is larger in the NCEP ensemble. Third, the spread of ECMWF usually becomes larger than NCEP for 3-day forecasts. This likely arises due to the differences of the energy growth between ECMWF and NCEP. While ECMWF starts from relatively small amplitudes of initial perturbations, the growth of the perturbations help to amplify the ensemble spread of tracks. On the other hand, the relatively large amplitudes of initial perturbations seem to play a role in producing the ensemble spread of tracks in NCEP.

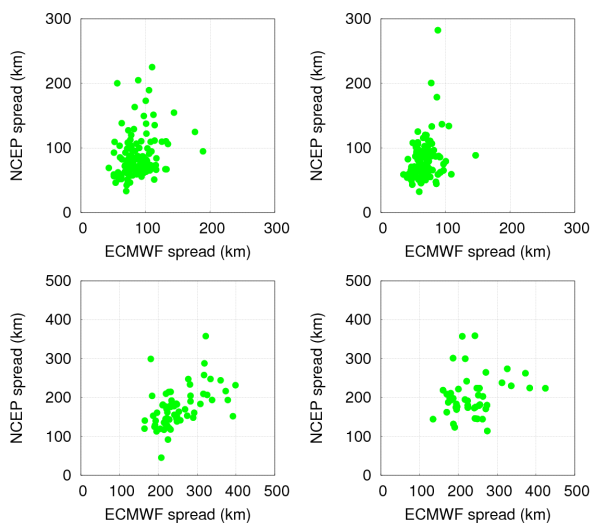


Fig. 7. Relationship of the spread of ensemble track forecasts between the ECMWF and NCEP ensembles for 24-h (top) and 72-h (bottom) forecasts in 2007 (left) and 2008 (right). Each dot in the figures shows the ensemble spread for each forecast event.

3. CONCLUSIONS

Ensemble initial perturbations and their growth were investigated in order to understand the ensemble spread of tracks. Using the recently established TIGGE database, vertical and horizontal distributions of initial perturbations around Typhoon Sinlaku (2008) were first compared among ECMWF, NCEP and JMA. It was found that the initial amplitude of NCEP wind perturbations was generally larger than that of ECMWF, particularly in the upper troposphere. For example, the 200 hPa NCEP perturbations were nearly 10 times as large as ECMWF in the before-recurvature stage of Sinlaku. Accordingly, the modification of the advection vector by the initial perturbations was larger in the NCEP ensemble than the ECMWF ensemble. JMA's perturbations were characterized by the large amplitude of specific humidity, which was nearly 4 times as large as NCEP at 925-hPa in the before-recurvature stage (not shown). In contrast, the JMA wind perturbations were small, being only a quarter the size of ECMWF at 700-hPa prior to recurvature. The subsequent growth of the advection flow of Sinlaku was found to be generally larger in ECMWF than NCEP. The dynamical perturbation growth in the ECMWF ensemble was found to be associated with 1) baroclinic energy conversion in a vortex, 2) baroclinic energy conversion associated with mid-latitude waves, and 3) barotropic energy conversion in a vortex. For baroclinic energy conversion in the vortex, the temperature perturbation is 90 degrees ahead of the streamfunction perturbation so that the perturbation can obtain the eddy available potential energy from the mean available potential energy, leading to the modification of the steering and asymmetric propagation vector. As previously studied, the baroclinic energy conversion associated with the mid-latitude waves caused the change in the steering flow. In addition, the radial eddy momentum flux near the center of Sinlaku was larger in the ECMWF ensemble than the NCEP ensemble. This barotropic process would result in the difference of the growth of the asymmetric propagation vector between them. A statistical verification demonstrated that NCEP's spread for 1-day forecasts was larger than ECMWF on average, likely due to the relatively large initial perturbation amplitudes and the accordingly large modification of the steering flow at the initial time. For 3-day forecasts, however, the spread of ECMWF became larger than that of NCEP, due to the larger energy growth in ECMWF. In summary, it appears that though

the ECMWF initial perturbation amplitudes are small, the growth of the perturbations help to obtain an appropriately large ensemble spread of tracks. Meanwhile, the relatively large amplitudes of initial perturbations seem to play a role in obtaining the ensemble spread of tracks in NCEP. Those results are comparable to those of Magnusson et al. (2008), who compared the skill of two versions of the ECMWF EPS: one based on SVs and the other based on bred vectors (BVs). They found that the initial amplitude of BVs needed to be amplified significantly to secure a sufficient ensemble forecast spread while the growth of SVs, whose amplitude is on the order of analysis error, played an important role in the SV-based EPS.

ACKNOWLEDGEMENT

The author would like to thank Dr. Sharanya J. Majumdar and Dr. David S. Nolan of the University of Miami, and Dr. Melinda S. Peng and Dr. Carolyn A. Reynolds of the Naval Research Laboratory for their helpful comments on this study. The author also thanks Dr. Sun-Hee Kim and Dr. Joe Kwon of Kongju National University in Korea for proving the Lanczos filtering program to compute the steering flows of TCs.

This study was conducted under the support of Office of Naval Research Grant Number N000140810250.

REFERENCES

- Carr, L. E. III, and R. L. Elsberry, 1992: Analytical tropical cyclone asymmetric circulation for barotropic model initial conditions. *Mon. Wea. Rev.*, **120**, 644-652.
- Fiorino, M., and R. L. Elsberry, 1989: Some aspects of vortex structure related to tropical cyclone motion. *J. Atmos. Sci.*, **46**, 975-990.
- Magnusson, L., M. Leutbecher, and E. Kallen, 2008: Comparison between Singular Vectors and Breeding Vectors as Initial Perturbations for the ECMWF Ensemble Prediction System. *Mon. Wea. Rev.*, **136**, 4092-4104.
- Yamaguchi, M., and S. J. Majumdar, 2010: Using TIGGE data to diagnose initial perturbations and their growth for tropical cyclone ensemble forecasts, *Mon. Wea. Rev.*, In Press.